Coordination of a bis-histidine-oligopeptide to Re(I) and Ga(III) in aqueous solution.

Gaetano De Tommaso[1], Gaetano Malgieri[2], Lucia De Rosa[3], Roberto Fattorusso[2, 5], Gianluca D'Abrosca[2], Alessandra Romanelli[4], Mauro Iuliano[1], Luca Domenico D'Andrea[3] and Carla Isernia*[2, 5].

1) Department of Chemical Sciences, University of Naples "Federico II" Cupa Nuova Cintia, 21–80126 Naples (ITALY).

2) Department of Environmental, Biological and Pharmaceutical, Sciences and Technologies, University of Campania "L. Vanvitelli", Via Vivaldi, 43–81100 Caserta (Italy)

3) Institute of Biostructure and Bioimaging, CNR, Via Mezzocannone, 16–80134 Naples (ITALY).

4) Department of Pharmaceutical Sciences, University of Milan, Via Venezian 21 - 20133 Milan (Italy)

5) Interuniversity Research Centre on Bioactive Peptides, Via Mezzocannone, 16–80134 Naples (Italy)

*Corresponding author:

Carla Isernia, carla.isernia@unicampania.it

Keywords:

Radiolabeled peptides, Rhenium(I), Gallium(III), potentiometry, NMR spectroscopy.

Abstract

The utilization of isotopes of transition metals for the development of novel therapeutic or diagnostic compounds is limited by the fact that they must be stabilized by chelating systems in coordination complexes. Important roles in the targeting approach are played by the tricarbonyl complexes of Technetium(I) and Rhenium(I) because they can be readily conjugated to biomolecules to form stable probes. Additionally, ^{67}Ga and ^{68}Ga isotopes of gallium are considered an obvious alternative to ^{99m}Tc[1111111] for SPECT and PET applications.

We have previously reported the characterization of the peptide CCK8 decorated with a *bis*-histidine-based chelator (pHis2) labeled with ^{99m}Tc-tricarbonyl.

In order to study the molecular properties of the histidine-based chelator pHis2, we here present the characterization in solution of its complexes with the metals Re(I) and Ga(III) using potentiometry and NMR. We detail the solution equilibria reporting pHis2 acid-base behavior, the coordination properties of pHis2 toward *fac*–$[Re(H_2O)_3(CO)_3]^+$ and Ga(III) and the atomic details of the formed complexes. Interestingly, two different metal coordination modes were found highlighting the plasticity of this bifunctional chelator.

Introduction

Radiolabeled peptides are useful compounds to be exploited for the diagnosis and therapy of a variety of human diseases characterized by overexpression of peptide cognate receptors. These molecules are usually composed by the targeting molecule (peptide moiety), a linker and a bifunctional ligand which binds to the radioactive metal. Several radiometals are being used in nuclear medicine such as $^{99m}Tc/^{188}Re$ which Tc(I)- or Re(I)-complexes $[Tc(H_2O)_3(CO)_3]^+$ (abbreviated as TcCO) or $[Re(H_2O)_3(CO)_3]^+$ (abbreviated as ReCO) could be prepared through a mild synthetic procedure[2]. In these complexes the water molecules can be replaced by ligands to obtain d^6 low spin complexes. Ligands replacing all water molecules can form very stable complexes, avoiding trans-chelation reactions, which may occur *in vivo,* and the generation of free metal. Between several ligands for Tc(CO)/Re(CO) that have been reported[3], special interest assume chelator moieties based on histidine side-chain as the imidazole ring is a good ligand for Tc(I)/Re(I) because of the aromatic sp^2 amine function. Several histidine–based chelating units have been reported so far. Earlier, it was shown that His positioned at the N-terminus of a peptide acts as convenient bidentate ligand[4]. To fully exploit the coordination properties of His as multidentate ligand, diverse His derivatives have been appended to the N-terminal peptide region[4-7]. To take advantage of the avidity phenomenon, modules with multiple histidines have been reported. His-tag appended to a protein of interest[8, 9] or his-his dipeptide[10] have been labeled respectively with TcCO and ReCO. Finally, tag composed of repetitive His-X dipeptides, such as HEHEHE-tag, have been described[11, 12]. We reported the *in vitro* and *in vivo* characterization of the peptide CCK8 decorated with a *bis*-histidine-based chelator (pHis2) and labeled with ^{99m}Tc-tricarbonyl[13]. The compound showed a specific high affinity binding to CCK2R receptors *in vivo* and cellular internalization. In imaging experiments, while concentration of the compound in the CCK2R positive tumors could be appreciated, there was poor contrast between target and non-target areas mainly due to accumulation in kidney and liver[13].

In order to shed light on the coordination properties of the bifunctional ligand we characterize in solution the complex between the metal Re(I) and the histidine-based chelator pHis2. In particular, we analyze the chemistry in aqueous solution and the molecular properties of pHis2 complexed to ReCO using NMR and potentiometry.

Furthermore, we also exploited the complexation of pHis2 with Ga(III), as isotopes of gallium, including ^{67}Ga for SPECT and ^{68}Ga for PET, are considered an obvious alternative to ^{99m}Tc[1]. The coordination chemistry of Ga(III) cation is dominated by functional groups like carboxylate, phosphonate, hydroxamate and amine. Gallium is mainly complexed using linear or macrocyclic polydentate chelator possessing hard donor groups (for example DTPA, NOTA, DOTA, deferoxamine), but an imidazole-based chelator has been also reported[14]. To analyze the chemistry in aqueous solution of Ga(III) cation complexed with aromatic amine, Ga(III)-His and Ga(III)-pHis2 complexes were characterized in aqueous solution by NMR and potentiometry. Interestingly, the Re(I) and Ga(III) metal ions show different binding mode to the pHis2 peptide. The structural and coordination differences have been determined revealing an unexpected molecular plasticity of the pHis2 unit.

Experimental section

Materials and methods

All amino acids and coupling reagents (HOBT and HBTU) were acquired from Novabiochem (Laüfelfingen, Switzerland), N,Ndimethylformamide (DMF) from Lab-Scan (Dublin, Ireland), DIPEA and trifluoroacetic acid (TFA) from Romil (Cambridge, UK), acetic anhydride from Applied Biosystem. Dichloromethane, Piperidine, 1,2-ethandithiol (EDT) were obtained from Fluka (Steinheim, Germany), triisopropylsilane from Aldrich (Steinheim, Germany). Acetonitrile HPLC grade was from Riedel-de Haën (Schnelldorf, Germany).

Dilute solutions of perchloric acid were prepared from Merck p.a. products and standardized potentiometrically (glass electrode) against tris(hydroxymethyl)amino methane (Aldrich) recrystallized from water twice and dried over conc. H_2SO_4 in *vacuo*. The acid concentration was checked by coulometry. The results agreed to within 0.1% or better.

Sodium hydroxide solutions, CO_2–free, were obtained by centrifugation of 50% "oil" as described in an earlier publication[15]. To prevent air contact the tubes were closed with a suba seal rubber. An approximately known quantity of NaOH was withdrawn with syringe and, at once, transferred under nitrogen atmosphere, in a calibrated volumetric flask containing $NaClO_4$ in the desired quantity, freshly boiled bidistilled water and soon brought to the mark. The accurate hydroxide concentration was determined by titration with HCl using methyl–red as a visual indicator. The analyses agreed to within 0.1%.

Sodium perchlorate source was the Merck p.a. $NaClO_4 \cdot H_2O$. Solutions 6 molal of the salt contain less than 10^{-5} molal concentration of iron, silica, heavy metals chloride and sulphate ions. Stock solutions were analyzed gravimetrically by drying at 130° C.

Gallium perchlorate, $Ga(ClO_4)_3 \cdot 6H_2O$, source was the Sigma Aldrich.

Nitrogen gas was taken from commercial cylinders and was purified by passing it through 10% H_2SO_4, 10% NaOH water and the ionic medium.

$^{2}H_2O$ (99.9% relative isotopic abundance) was purchased from Cambridge Isotope Laboratories.

Synthesis of *fac*–$[Re(H_2O)_3(CO)_3]^+$

fac-$[Re(H_2O)_3(CO)_3]^+$ was prepared starting from Rhenium(I) pentacarbonyl chloride (Aldrich) as already reported [16,17].

Synthesis of the peptide chelator and its analogues

pHis2 (H-Lys(His)-βAla-Lys(His)-NH_2), Ac-pHis2 (Ac-Lys(His)-βAla-Lys(His)-NH_2) and Ac3-pHis2 (Ac-Lys(Ac^{α}-His)-βAla-Lys(Ac^{α}-His)-NH_2) were synthesized on solid phase by standard Fmoc chemistry on the Rink Amide PEG-MBHA resin (0.54 mmol/g, Iris Biotech) performing the deprotection steps by incubation with 30% piperidine in dimethylformamide (DMF) (2 x 5 min), coupling reactions with a 10-fold excess of Fmoc-protected amino acid (Iris Biotech), 10 eq of COMU and 20 eq of N,N-Diisopropylethylamine (DIPEA) (1 x 30 min) and washes with DMF. The lysine residues were introduced as N-α-Fmoc-N-ε-4-methyltrityl-L-lysine (Iris Biotech). After the assembling of the linear chain, N-ε-4-methyltrityl-L-lysine residues were deprotected by treatment with a solution of trifluoroacetic acid (TFA, Sigma-Aldrich), triisopropylsilane (TIS, Sigma-Aldrich) and dichloromethane (DCM, Sigma-Aldrich) 1/5/94 v/v/v (1 x 1 min with the solution of TFA/TIS/DCM and 3 x 1 min with DCM, repeated 10 times). Then, Fmoc-His(trt)-OH was coupled on the side-chain of the Lys residues, using 20 eq of the Fmoc-protected amino acid, 20 eq of COMU and 40 eq of DIPEA (30 min). Ac-pHis2 was selectively acetylated on N-terminal α-amino group of Lys after linear peptide assembly deprotecting the Fmoc group and using a solution of 2 M acetic anhydride, 0.55 M DIPEA, 0.06 M HOBt in NMP (5 min). Peptide Ac_3-pHis2 was acetylated on N-terminal α-amino groups after full Fmoc deprotection by incubation with 30% piperidine in DMF (2 x 5 min) and acetylation by treatment with a solution of 2 M acetic anhydride, 0.55 M DIPEA, 0.06 M HOBt in NMP (10 min).

Peptides were cleaved off the resin by incubation with a solution of TFA/TIS/H_2O (95/2.5/2.5) (3 h, at room temperature, under stirring) and precipitated in cold diethyl ether. Peptides were finally purified by RP-HPLC on an Axia Synergi 4µ MAX-RP, 80 Å, 50 x 21.2 mm column applying a gradient of CH_3CN (0.1% TFA) in H_2O (0.1% TFA) from 1% to 40% in 20 min. Analytical characterization by RP-HPLC of peptides was carried out using a column Jupiter Proteo 150 x 4.6 mm, 90 Å, 4 µ (Phenomenex), applying a gradient of CH_3CN (0.1% TFA) in H_2O (0.1% TFA) from 1% to 40% in 20 min (Figure S1). The purity of all peptides was greater than 95% and was estimated by RP-HPLC evaluating the area of the chromatographic peaks revealed at 210 nm. Peptides were identified by ESI ToF mass analysis

pHis2: MW_{th}= 618.36 Da, MW_{exp}= 618.37 Da

Ac-pHis2: MW_{th}= 660.37 Da, MW_{exp}= 660.37 Da

Ac3-pHis2: MW_{th}= 744.39 Da, MW_{exp}= 744.40 Da.

Potentiometry

The potentiometric titrations were performed in an air-bath thermostat kept at (25.00 ± 0.05) °C.

A programmable computer controlled data acquisition unit 3421A, supplied by Hewlett and Packard, was used to perform the potentiometric measurements.

The glass electrodes were Metrohm of 60102-100 type and Ag/AgCl electrode was utilized as reference. The EMF values were measured with a precision of ± 0.01 mV using a Keithley 642 type Digital Electrometer.

UV/CD spectra were recorded by model J–715 JASCO spectropolarimeter, from 200 to 400 nm (optical path 1.00 cm) at 25.0 °C, under a constant flow of nitrogen.

NMR analysis

All the NMR spectra were recorded at 298 K on a Varian Unity spectrometer operating at a proton frequency of 500 MHz, located at the Department of Environmental, Biological and Pharmaceutical, Science and Technologies, in Caserta (Italy).

For the titrations with *fac*–$[Re(H_2O)_3(CO)_3]^+$ or Ga(III) (each used as 8 mM bulk solutions) each sample was individually prepared utilizing 4 mM bulk solutions of pHis2 containing 10% D_2O. 1D spectra, acquired with 16K and zero-filled to 32 K data points, were obtained for each of the following *fac*–$[Re(H_2O)_3(CO)_3]^+$/pHis2 molar ratios: 0/1, 0.2/1, 0.5/1, 1/1, 1.5/1.

The proton chemical shifts were collected at 298 K, at pH = 5.8, and referenced to external TMS (δ = 0 ppm). Two-dimensional phase-sensitive TOCSY, NOESY and ROESY spectra [18] were collected using the States and Haberkorn method. TOCSY, NOESY and ROESY experiments were recorded with mixing times of 70, 200 and 150 ms, respectively. Water suppression, when necessary, was achieved using the DPFGSE sequence [19]. Typically, 64 transients of 4K data points were collected for each of the 256 increments; the data were zero filled to 1K in ω1. Squared shifted sine-bell functions were applied in both dimensions prior to Fourier transformation and baseline correction. The data were processed and analyzed using the VNMRJ and CARA software [20].

Results and Discussion

Potentiometric studies

Acid–base behavior of pHis2 chelator

pHis2 ligand, according to the structure (Fig. 1), has five groups that in acid solution are completely protonated giving the H_5L^{5+} form.

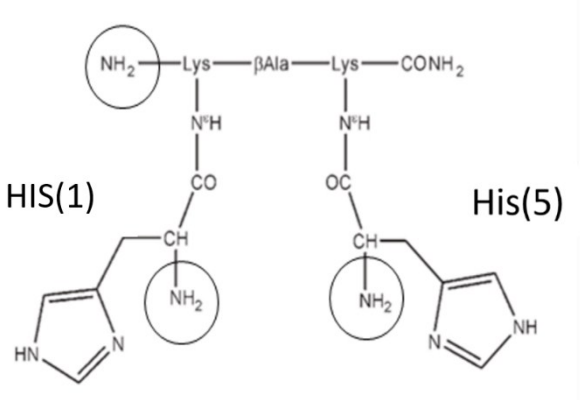

Fig.1. Structure of the bifunctional chelator (pHis2) and related sites of acetylation.

The acid–base equilibria are described by the general equation:

$$H_{6-p}L^{(6-p)+} + H_2O = H_{5-p}L^{(5-p)+} + H_3O^+ \qquad K_{Ap} \qquad (1 \le p \le 5) \qquad (1)$$

The determination of the protolysis constants is carried out by potentiometric titration at a temperature of 25° C in 0.1 M $NaClO_4$ as ionic medium. The solutions analyzed have the following composition:

$$\text{TS: } C_L \text{ M pHis2, } C_A \text{ M } HClO_4, C_B \text{ M NaOH, } (0.1 - C_A) \text{ M } NaClO_4$$

In the test solutions, the concentration of pHis2, ranged from $1.0 \cdot 10^{-3}$ to $4.0 \cdot 10^{-3}$ M, while the proton excess, $C_H = (C_A - C_B)$ is between $2.0 \cdot 10^{-4}$ and $-7.0 \cdot 10^{-3}$ M.

The measurement of the hydrogen ion concentration, $h = [H_3O^+]$, is carried out by using the following cell:

$$\text{GE / TS / RE} \qquad (A)$$

where GE represents the glass electrode, while RE is the reference half–cell:

$$RE = 0.1\ M\ NaClO_4 / 0.01\ M\ AgClO_4, 0.09\ M\ NaClO_4 / AgCl_{(s)} / Ag_{(s)}$$

The e.m.f. of the cell (A) at a temperature of 25° C results:

$$E_G = E_G' + 0.05916 \cdot \log (h \cdot y_H) + E_J \qquad (2)$$

where E_G' is a constant in each titration and y_H represents the activity coefficient of H^+ ion, constant at a given value of ionic strength (I). The quantity E_J represents the liquid junction potential which is generated at the contact between the 0.1 M $NaClO_4$ solution and the measurement solution[21]. This quantity depends on the hydrogenionic concentration according to the equation[22];

$$E_J = -0.51 \cdot h + 0.24 \cdot K_w/h \qquad (3)$$

The E_G values are recorded when a constant potential value is reached ($\pm 0.05 \cdot 10^{-3}$ V/h). Placing:

$$E_G^\circ = E_G' + 0.05916 \cdot \log (y_H) \qquad (4)$$

the equation (2) becomes:

$$E_G = E_G^\circ + 0.05916 \cdot \log h + E_J \qquad (5)$$

Each titration is conducted into two parts: in the first one the constant E_G° is determined in a solution in the absence of a ligand, reducing the acidity by adding a solution of NaOH of known concentration, up to $C_H = 5.0 \cdot 10^{-5}$ M. In the second part, the peptide is added and the alkali solution is added, measuring the hydrogen ion concentration.

From experimental data (C_L, C_H, $[H^+]$) the average number (Z_H) of protons released per molecule of peptide, is evaluated by:

$$Z_H = ([H^+] - C_H - K_w/[H^+])/C_L$$

where a value $K_w = 10^{-13.78}$ was utilized. Reporting Z_H as function of pH (Fig.2) values p from 1 to 5 are obtained.

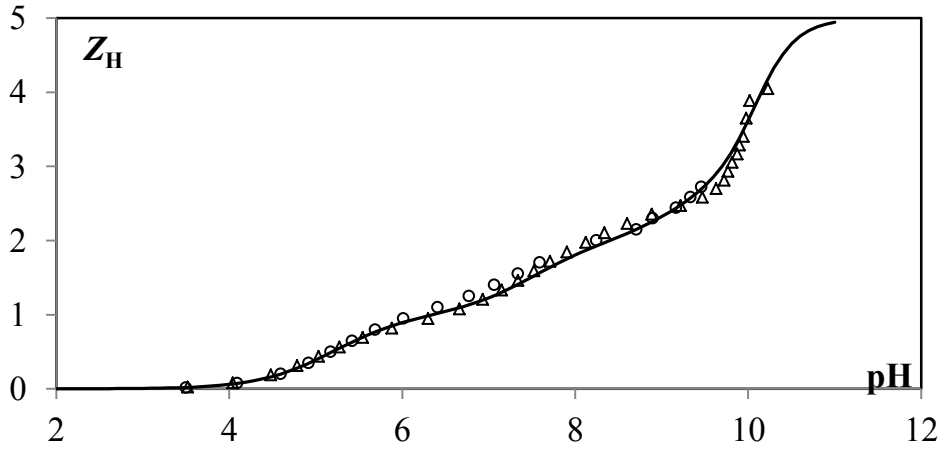

Fig.2. Z_H as function of pH in 0.1 $NaClO_4$ for the H_5L^{5+} system. The triangles indicate measurements obtained with $C_L = 2.9 \cdot 10^{-3}$ M, while the circles represent return data. The solid line is obtained with constant values: log $K_{A1} = -5.35$, log $K_{A2} = -7.45$, log $K_{A3} = -9.3$, log $K_{A4} = -10.3$, log $K_{A5} = -10.5$.

A speciation model is obtained by processing the experimental data using *Hyperquad* program[23].

In order to attribute the constants to each group, measurements were performed on modified peptides, in which some amino groups are acetylated. In particular, we synthesized a mono-acetylated analog of pHis2 (Ac-pHis2) presenting the acetyl group on the α-amino group of Lys2 and a tri-acetylated analog of pHis2 (Ac_3-pHis2) presenting the acetyl groups on the α-amino group of Lys2, His1 and His5(Fig.1).

The obtained results are summarized in the Table 1, the species distribution diagram is given in Fig.3.

Tab.1. Acid constants of the pHis peptide and its acetylated analogs in 0.1 M $NaClO_4$.

$$H_{6-p}L^{(6-p)+} + H_2O = H_{5-p}L^{(5-p)+} + H_3O^+ \qquad pK_{Ap} \pm 3\sigma$$

Peptide	pK_{A1} (His)	pK_{A2} (His)	pK_{A3} (NH_2–His)	pK_{A4} (NH_2–His)	pK_{A5} (NH_2–Lys)
pHis2	5.35 ± 0.05	7.45 ± 0.05	9.3 ± 0.1	10.3 ± 0.2	10.5 ± 0.3
Ac–pHis2	5.40 ± 0.05	7.50 ± 0.05	9.2 ± 0.1	10.4 ± 0.2	–
Ac_3–pHis2	6.25 ± 0.05	8.75 ± 0.05	–	–	–

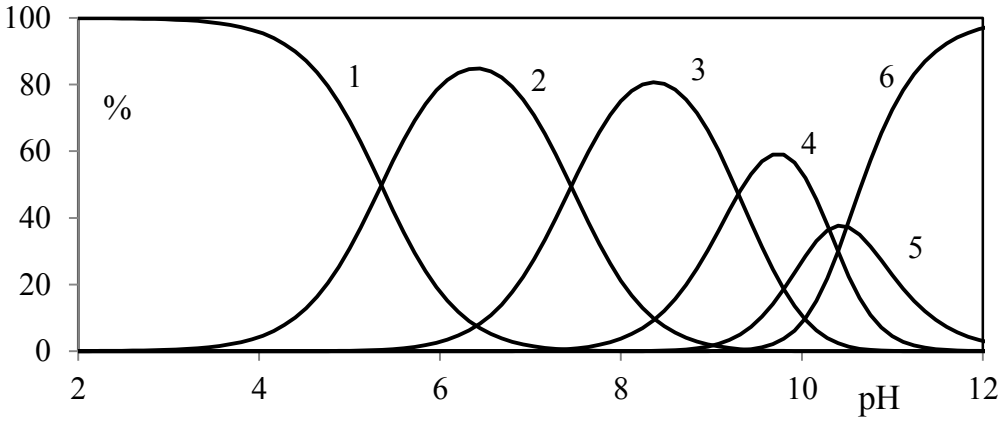

Fig.3. Acid–base distribution diagram of peptide chelator pHis2 in 0.1 M $NaClO_4$ with $C_L = 2.0\cdot10^{-3}$ M (1: H_5L^{5+}; 2: H_4L^{4+}; 3: H_3L^{3+}; 4: H_2L^{2+}; 5: HL^{+}; 6: L).

Complexation of *fac*–$[Re(H_2O)_3(CO)_3]^+$ and Ga^{3+} ions with peptide pHis2 in 0.1 M $NaClO_4$

The coordination properties of pHis2 (H_5L^{5+}) toward *fac*–$[Re(H_2O)_3(CO)_3]^+$ and Ga^{3+} (Me^{n+}) ions can be written in the form:

$$Me^{n+} + q\ H_5L^{5+} = MeH_{-p}L_q^{(n-p)} + (5q + p)\ H^+ \quad \beta_{q,-p} \qquad (6)$$

The measurements are carried out as potentiometric titrations where the hydrogen ion concentration is determined by the e.m.f. of cell (A):

$$(-)\ \text{RE/Test Solution/GE}\ (+) \qquad (A)$$

in which GE symbolizes glass electrode and RE is the reference half–cell:

RE = 0.1 M $NaClO_4$/0.01 M $AgClO_4$, 0.09 M $NaClO_4$/AgCl/Ag

The test solutions have the general composition:

TS_{Re} = C_{Me} M MeCl, C_L M pHis2, C_A M $HClO_4$, C_B M NaOH, (0.1 − C_A) M $NaClO_4$

TS_{Ga} = C_{Me} M $Me(ClO_4)_3$, C_L M pHis2, C_A M $HClO_4$, C_B M NaOH, (0.1 − C_A − 3C_M) M $NaClO_4$

The concentration of the ligand is varied between $2.0\cdot10^{-3}$ M and $8.0\cdot10^{-3}$ M, while for both metal ions the concentration, C_{Me}, is between $1.0\cdot10^{-3}$ M and $3.0\cdot10^{-3}$ M.

The proton excess, $C_H = (C_A - C_B)$, varies in the interval $-5.0\cdot10^{-3}$ and $5.0\cdot10^{-3}$ M.

fac–$[Re(H_2O)_3(CO)_3]^+$)–pHis2 system

In a previous work[17] the hydrolysis products of Rhenium(I) cation were evaluated.

From experimental data (C_{Me}, C_L, C_H, $[H^+]$) obtained in solutions containing different *fac*−$[Re(H_2O)_3(CO)_3]^+$) and peptide ratio, the average number of protons Z_L released by complexing is given that:

$$Z_L = ([H^+] - C_H - K_w/[H^+])/C_L$$

($K_w = 10^{-13.78}$ is water ionic product). Variation of Z_H (pH) function is observed (Fig.4) with respect free peptide, as a consequence of complexation of the Rhenium(I) cation.

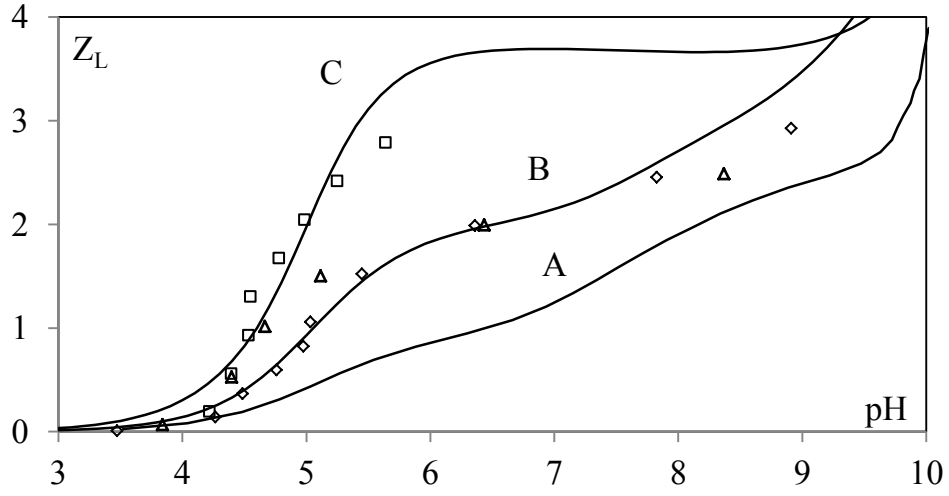

Fig.4. Z_L as function of pH for the H_5L^{5+} system (A) and Re(I)−L system in 0.1 $NaClO_4$ in solutions with C_{Me}/C_L ratio: 1.0 (diamonds and triangles) (B), 2.0 (squares) (C). The solid lines are obtained with the constants reported in Tab.2.

Ga^{3+}−pHis2 system

Potentiometric measurements are carried out both with ligand precursor, such as histidine, and the pHis2. For both systems a complexing effect is observed.

The determination of equilibrium constants is obtained by evaluating Z_M:

$$Z_M = ([H^+] - C_H - K_w/[H^+])/C_{Me}$$

The results are shown in Fig.5 and Fig.6.

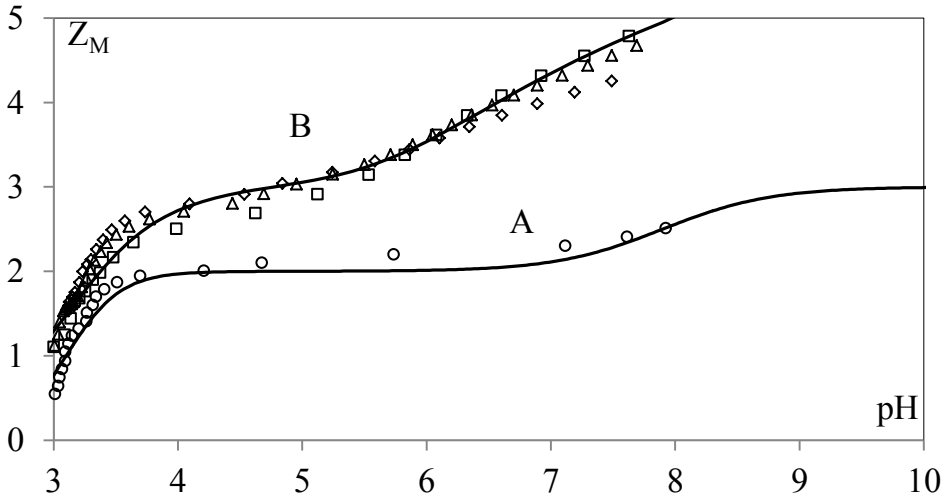

Fig.5. Z_M as function of pH for Ga(III) hydrolysis system ($C_{Me} = 4.8 \cdot 10^{-3}$ M) (A) and Ga(III)−His system in 0.1 $NaClO_4$ in solutions with C_{Me}/C_L ratio: 1.0 (diamonds), 0.5 (triangles and squares) (B). The solid lines are obtained with the constants reported in Tab.2.

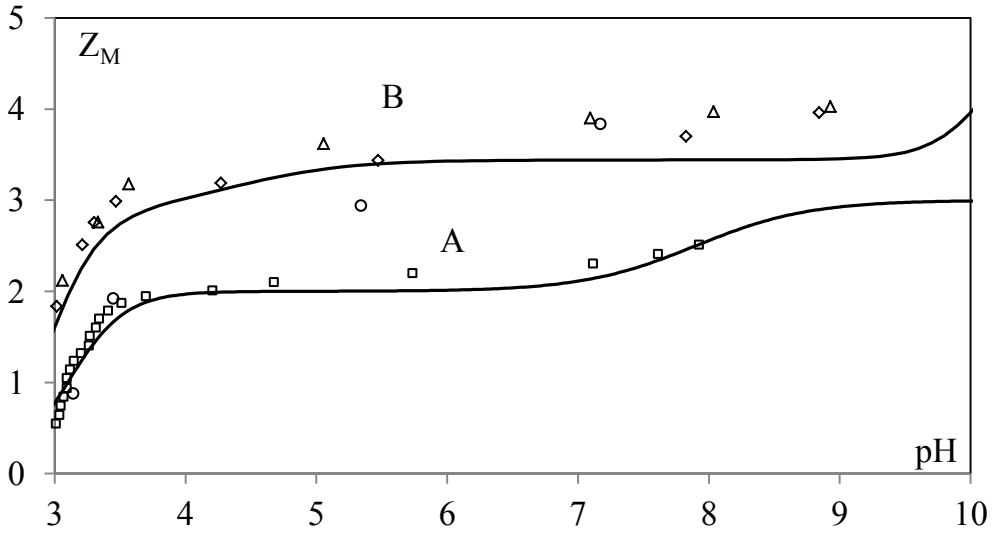

Fig.6. Z_M as function of pH for Ga(III) hydrolysis system ($C_{Me} = 4.8 \cdot 10^{-3}$ M) (A) and Ga(III)−pHis2 system in 0.1 $NaClO_4$ in solutions with C_{Me}/C_L ratio: 1.0 (diamonds and circles), 2.0 (triangles) (B). The solid lines are obtained with the constants reported in Tab.2.

Elaboration of data

The data collected are elaborated with the HYPERQUAD program[23], where are included the Gallium hydrolysis constants, obtained experimentally, and the *fac*−$[Re(H_2O)_3(CO)_3]^+$ complex reported in the literature[17, 24].

In the table are summarized the results obtained:

Tab.2. Equilibrium constants for Ga(III) hydrolysis system and Ga(III)−His, Ga(III)−pHis2 and Me^{+}−pHis2. (Me^{+}: *fac*–$[Re(H_2O)_3(CO)_3]^{+}$)

Equilibria	log(equil. cost.) ± 3σ
$Ga^{3+} + 2\ H_2O = Ga(OH)_2^{+} + 2\ H^{+}$	−6.2 ± 0.8
$Ga^{3+} + 3\ H_2O = Ga(OH)_3 + 3\ H^{+}$	−14.1 ± 0.6
$Ga^{3+} + HHis^{+} + 5\ H_2O = Ga(OH)_2His^{+} + 3\ H_3O^{+}$	−6.82 ± 0.09
$Ga^{3+} + H_5L^{5+} + 6\ H_2O = Ga(OH)_2H_3L^{4+} + 4\ H_3O^{+}$	−9.69 ± 0.16
$Me^{+} + H_5L^{5+} + 2\ H_2O = MeH_3L^{4+} + 2\ H_3O^{+}$	−7.07 ± 0.04

To visualize the amounts of the different species, distribution diagram is constructed for Rhenium(I)–pHis2 system (Fig.7), Gallium(III)–His (Fig.8 and Fig.S2) and Gallium(III)–pHis2 (Fig.9 and Fig.S3) .

For Rhenium(I)–pHis2 system, it is observed that the complex $Re(CO)_3H_3L^{4+}$ reaches a concentration greater than 60% in a pH range between 6 and 8.

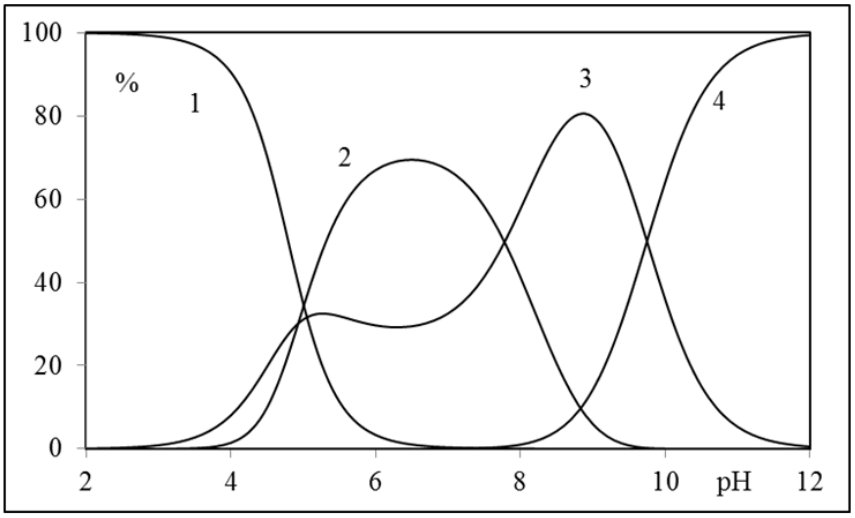

Fig.7. Distribution diagram of *fac*−$[Re(H_2O)_3(CO)_3]^{+}$−pHis2 system in 0.1 M $NaClO_4$ with $C_{Re(CO)3+}$ = $1.0\cdot10^{-3}$ M and $C_L = 2.0\cdot10^{-3}$ M (1: $Re(CO)_3^{+}$; 2: $Re(CO)_3H_3L^{4+}$, 3: $ReH_{-1}(CO)_3$; 4: $ReH_{-2}(CO)_3^{-}$).

From the distribution diagram of the Ga (III)–His system (ratio 1:1), shown in Fig.8, a prevalence of free metal and $Ga(OH)_2^{+}$ species is observed up to a pH of around 3, while in the pH range between 4 and 6 there is a prevalence of the $Ga(OH)_2His^{+}$ complex which reaches a maximum of 60%. For pH greater than 7, on the other hand, the $Ga(OH)_3$ hydrolyzed form becomes significant. The increase in the C_L/C_{Me} ratio, as shown in the diagram in Fig.S2, involves an increase in the fraction of the $Ga(OH)_2His^{+}$ complex, which reaches a maximum of 80% in the range of pH 4–6.

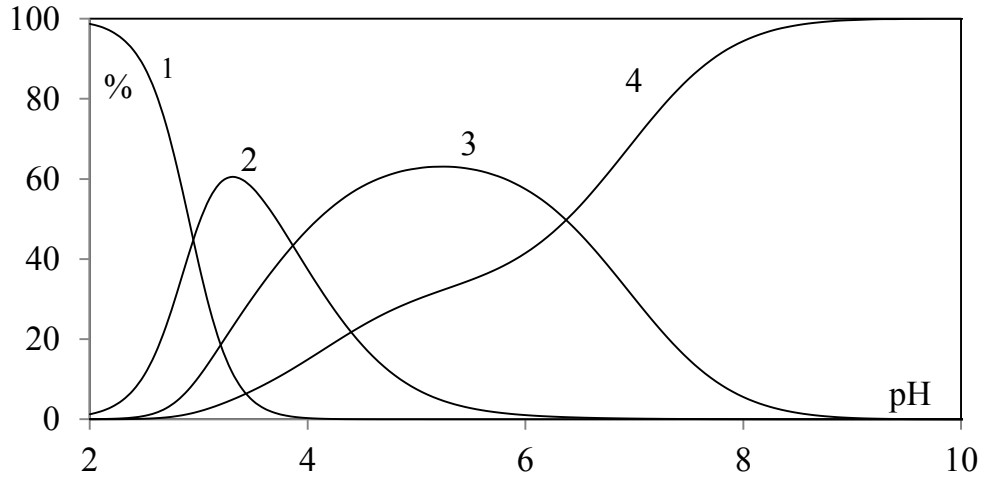

Fig.8. Distribution diagram of Ga(III)–His system in 0.1 M $NaClO_4$ with $C_{Me} = C_L = 2.0 \cdot 10^{-3}$ M (1: Ga^{3+}; 2: $Ga(OH)_2^+$, 3: $Ga(OH)_2His^+$; 4: $Ga(OH)_3$).

The distribution diagrams of the Ga(III)–pHis2 system, for different C_L/C_{Me} ratios, are shown in Fig.9 and Fig.S3. Compared to the Ga(III)–His system, a greater pH range (4–9) is observed in which the $Ga(OH)_2H_3L^{4+}$ complex predominates. For pH greater than 10 it becomes, also in this case, the contribution of the $Ga(OH)_3$ species.

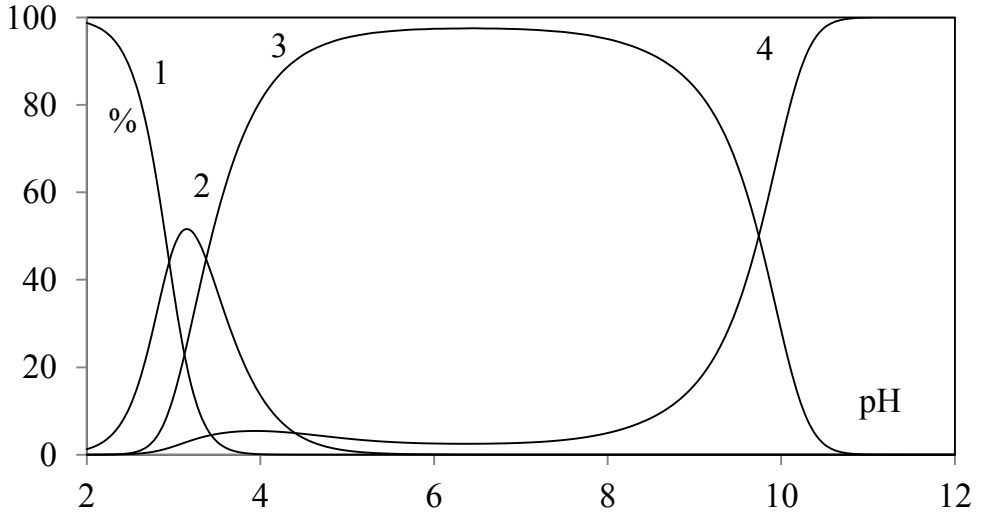

Fig.9. Distribution diagram of Ga(III)–pHis2 system in 0.1 M $NaClO_4$ with $C_{Me} = C_L = 2.0 \cdot 10^{-3}$ M (1: Ga^{3+}; 2: $Ga(OH)_2^+$, 3: $Ga(OH)_2His^+$; 4: $Ga(OH)_3$).

NMR Results

The formation of the complexes *fac*–$[Re(H_2O)_3(CO)_3]^+$/pHis2 and Ga(III)/pHis2 was followed in a short titration where the metal ion was added to a fixed concentration of the peptide chelator. The titration was made at pH = 5.8, since the *fac*–$[Re(H_2O)_3(CO)_3]^+$ compound was already characterized at this pH and its protonation constants are available[17]. For each point of the titration a

full set of mono and bidimensional experiments (Fig.S4) was acquired in order to follow the effect of the addition on the pHis2.

The full proton assignment of the pHis2 in H_2O at pH = 5.8 is reported in Table S1 of the Supplemental Material. Two diagnostic NOE signals allowed the sequential assignment of the backbone: NH-βAla3/Hα-His2, NH-Lys4/Hα-βAla3. It should be noted that the amine protons of His1, Lys2 and His5 are exchangeable in these conditions and thus are not visible in the spectra. Furthermore, as the system is highly symmetric only very weak differences are experimented by the chemical shifts of the two His and two Lys.

The formation of the coordination compound with rhenium is shown in Fig. 10, where a comparison of the 1D spectra of the free and the *fac*–$[Re(H_2O)_3(CO)_3]^+$/pHis2 1.5/1 species demonstrates that upon *fac*–$[Re(H_2O)_3(CO)_3]^+$ addition the formation of a complex occurs. In fact, the exchangeable NH protons of the two histidines become visible at 7.34 ppm in the complex and their peaks integral increases with the metal ion/peptide ratio. At the same time, the αCH protons of histidines moves from 4.07 ppm to 6.12 ppm while the βCH from 3.22 to 5.81. Interestingly, the imidazole signals of both histidines do not experience any change in chemical shifts, thus suggesting that only the terminal NHs are involved in the coordination[25, 26]. Accordingly, the potentiometric data indicate, in these conditions, the loss of two protons. This unexpected coordination mode has not yet been described in literature, whereas imidazole nitrogen has always supposed to be implicated in metal coordination[27, 28]. However, it should be noted that in general Tc(I)/Re(I) labeling conditions, unlike the conditions used in this work, involves the heating of the labelling mixture.

A completely different coordination mode is found when the peptide is titrated with Ga(III). Firstly, no change in the hydrodynamic properties of the peptide are observed in the DOSY spectra. pHis2 binds this latter ion by using the histidine side chains. In particular (figure 10), both imidazole signals (8.51 and 7.28 ppm) broaden and sensibly change their chemical shift toward higher fields upon metal ion addition[29, 30].

No multiplication of $H_{\delta 2}$ and $H_{\varepsilon 1}$ signals is observed in the spectra thus indicating the formation of a single tautomeric form in solution. The bigger chemical shift change of the $H\varepsilon_1$ suggests that the preferred tautomer should be the one with the N_δ protonated and the N_ε involved in the Ga(III) coordination[31, 32]. In the Ga(III)-pHis2 spectra, small chemical shift perturbations are observable also for the signals belonging to the lysine side chains. The same perturbations are not observable in the case of the complex with the *fac*–$[Re(H_2O)_3(CO)_3]^+$ thus suggesting a deeper embedment of the Ga(III) in the space defined by the two residues lysine side–chains. This behavior can find an explanation in the bigger steric hindrance of the *fac*–$[Re(H_2O)_3(CO)_3]^+$ complex.

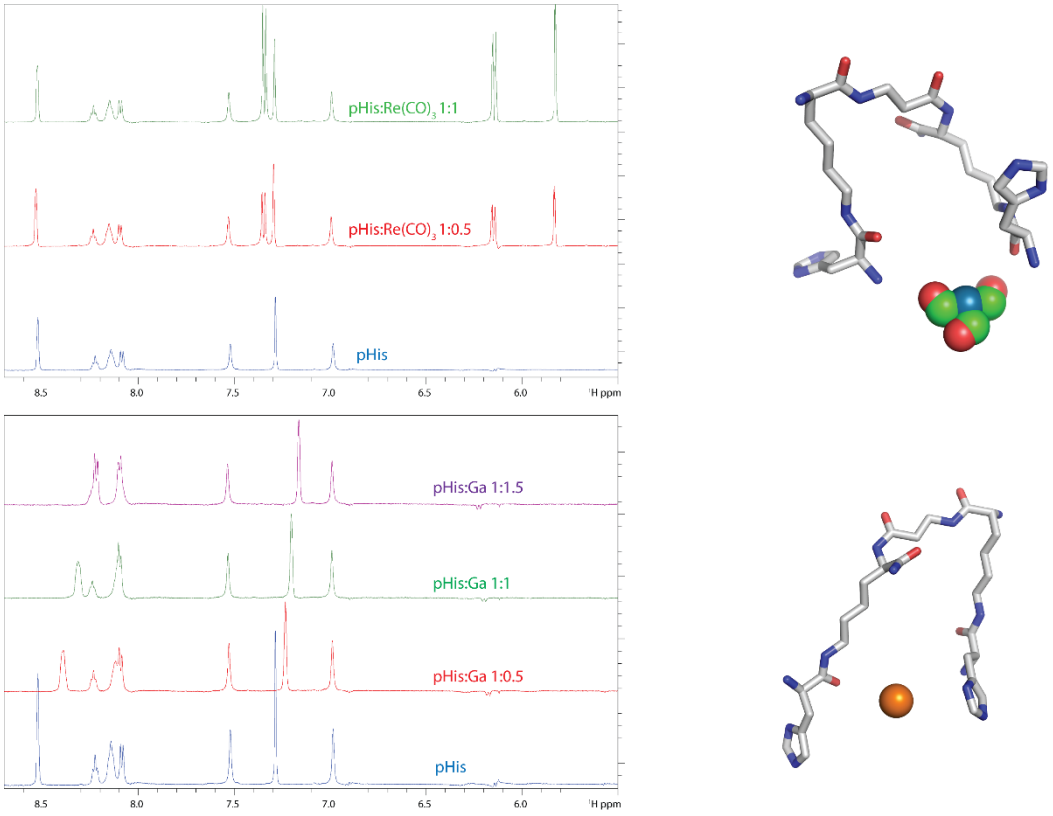

Fig. 10. ^{1}H NMR spectra obtained at different ratio of *fac*–$[Re(H_2O)_3(CO)_3]^+$/pHis2 (upper left) and of Ga(III)/pHis2 (lower left). Schematic cartoon of *fac*–$[Re(H_2O)_3(CO)_3]^+$–pHis2 (upper right) and Ga(III)–pHis2 (lower right) complexes (see also Fig.S5).

By potentiometric data, the constants relative to formation of complexes are:

$$Me^+ + H_3L^{3+} = MeH_3L^{4+} \qquad K = 10^{12.5}$$

and

$$Ga(OH)_2^+ + H_3L^{3+} = Ga(OH)_2H_3L^{4+} \qquad K = 10^{16.1}$$

obtained with the constants in Table 2.

The Ga(III)–pHis2 complex has an higher formation constant than Me^+–pHis2 one in agreement with NMR results.

Conclusions

In the present work, we have spectroscopically analyzed the chemistry in aqueous solution and the properties of the histidine-based chelator pHis2 complexed to the *fac*–$[Re(H_2O)_3(CO)_3]^+$ and Ga(III) to unveil the molecular determinants of their coordination in order to contribute the

characterization of a novel peptide-based chelating unit that could be exploited for diagnosis and therapy.

Potentiometric and spectroscopic data agree in demonstrating how the peptide behaves in a complete different manner in the two cases. In the case of *fac*–$[Re(H_2O)_3(CO)_3]^+$ complexation, pHis2 uses the up two histidine N-terminal amine groups to coordinate a single metal group revealing an unexpected complex structure. In the case of Ga(III), the peptide uses the two histidine side chains to bind the metal ion. The metal coordination blocks the two histidines in a preferred tautomer with the N_δ protonated and the N_ε involved in the coordination. This different coordination mode is due to the bigger steric hindrance of the *fac*–$[Re(H_2O)_3(CO)_3]^+$ complex if compared to the steric hindrance of the simple Ga(III) metal ion.

As the selection of proper biomolecular ligands is indispensable in the design of novel radiopharmaceutical compounds, our study complements the literature data by describing in details the solution equilibria, the coordination properties, the constants of each equilibrium reaction and the atomic details of the formed complexes.

Conflicts of interest

There are no conflicts to declare.

Acknowledgements

This work was partially funded by MIUR PRIN grant no. 20157WZM8A to G.M. We thank Veronica Celentano for the help with peptide synthesis.

References

1. M. D. Bartholomä, A. S. Louie, J. F. Valliant and J. Zubieta, *Chem Rev*, 2010, **110**, 2903-2920.
2. R. Alberto, R. Schibli, E. Andrè, A. P. Schubiger, U. Abram and T. A. Kaden, *Journal of American Chemical Society*, 1998, **120**, 7987-7988.
3. R. Alberto, J. K. Pak, D. van Staveren, S. Mundwiler and P. Benny, *Biopolymers*, 2004, **76**, 324-333.
4. A. Egli, R. Alberto, L. Tannahill, R. Schibli, U. Abram, A. Schaffland, R. Waibel, D. Tourwé, L. Jeannin, K. Iterbeke and P. A. Schubiger, *J Nucl Med*, 1999, **40**, 1913-1917.
5. J. K. Pak, P. Benny, B. Spingler, K. Ortner and R. Alberto, *Chemistry*, 2003, **9**, 2053-2061.
6. R. Misri, K. Saatchi and U. O. Häfeli, *Nucl Med Commun*, 2011, **32**, 324-329.
7. D. Papagiannopoulou, C. Tsoukalas, G. Makris, C. Raptopoulou, V. Psycharis, L. Leondiadis, E. Gdniazdowska, P. Koźmiński, L. Fuks, M. Pelecanou, I. Pirmettis and M. Papadopoulos, *Inorganica Chimica Acta - INORG CHIM ACTA*, 2011, **378**, 333-337.
8. R. Waibel, R. Alberto, J. Willuda, R. Finnern, R. Schibli, A. Stichelberger, A. Egli, U. Abram, J. P. Mach, A. Plückthun and P. A. Schubiger, *Nat Biotechnol*, 1999, **17**, 897-901.
9. R. Tavaré, J. Williams, K. Howland, P. J. Blower and G. E. Mullen, *J Inorg Biochem*, 2012, **114**, 24-27.
10. R. S. Herrick, C. J. Ziegler and A. Gambella, *European Journal of Inorganic Chemistry*, 2010, **2010**, 3905-3908.
11. V. Tolmachev, C. Hofström, J. Malmberg, S. Ahlgren, S. J. Hosseinimehr, M. Sandström, L. Abrahmsén, A. Orlova and T. Gräslund, *Bioconjug Chem*, 2010, **21**, 2013-2022.
12. C. Hofström, M. Altai, H. Honarvar, J. Strand, J. Malmberg, S. J. Hosseinimehr, A. Orlova, T. Gräslund and V. Tolmachev, *J Med Chem*, 2013, **56**, 4966-4974.
13. L. D. D'Andrea, I. Testa, M. Panico, R. Di Stasi, C. Caracò, L. Tarallo, C. Arra, A. Barbieri, A. Romanelli and L. Aloj, *Biopolymers*, 2008, **90**, 707-712.
14. A. Schmidtke, T. Läppchen, C. Weinmann, L. Bier-Schorr, M. Keller, Y. Kiefer, J. P. Holland and M. D. Bartholomä, *Inorg Chem*, 2017, **56**, 9097-9110.
15. R. Porto, G. De Tommaso and E. Furia, *The Second Acidic Constant of Salicylic Acid*, 2005.
16. N. Lazarova, J. Babich, J. Valliant, P. Schaffer, S. James and J. Zubieta, *Inorganic Chemistry*, 2005, **44**, 6763-6770.
17. G. De Tommaso, V. Celentano, G. Malgieri, R. Fattorusso, A. Romanelli, L. D. D'Andrea, M. Iuliano and C. Isernia, *ChemistrySelect*, 2016, **1**, 3739-3744.
18. H. Kessler, M. Gehrke and C. Griesinger, *Two-Dimensional NMR Spectroscopy: Background and Overview of the Experiments [New Analytical Methods (36)]*, 1988.
19. T. L. Hwang and A. J. Shaka, *J Magn Reson Ser A*, 1995, **112**, 275-279.
20. C. Bartels, T. H. Xia, M. Billeter, P. Guntert and K. Wuthrich, *J Biomol Nmr*, 1995, **6**, 1-10.
21. C. H. Rochester, *Journal of the Chemical Society, Dalton Transactions*, 1972, 5-8.
22. G. Biedermann and L. G. Sillén, *Journal*, 1953, **5**, 425–540.
23. P. Gans, A. Sabatini and A. Vacca, *Talanta*, 1996, **43**, 1739-1753.
24. C. F. Baes and R. E. Mesmer, 1976.
25. G. Malgieri and G. Grasso, *Coordination Chemistry Reviews*, 2014, **260**, 139-155.
26. G. Malgieri, M. Palmieri, L. Russo, R. Fattorusso, P. V. Pedone and C. Isernia, *FEBS J*, 2015, **282**, 4480-4496.
27. K. E. Bullok, M. Dyszlewski, J. L. Prior, C. M. Pica, V. Sharma and D. Piwnica-Worms, *Bioconjug Chem*, 2002, **13**, 1226-1237.
28. Y. Ma, S. Liang, H. Wu and H. Wang, *Journal of Radioanalytical and Nuclear Chemistry*, 2014, **299**, 1865-1870.
29. A. Travaglia, G. Arena, R. Fattorusso, C. Isernia, D. La Mendola, G. Malgieri, V. G. Nicoletti and E. Rizzarelli, *Chemistry*, 2011, **17**, 3726-3738.
30. A. Travaglia, D. La Mendola, A. Magrì, A. Pietropaolo, V. G. Nicoletti, G. Grasso, G. Malgieri, R. Fattorusso, C. Isernia and E. Rizzarelli, *Inorg Chem*, 2013, **52**, 11075-11083.
31. G. Malgieri, M. Palmieri, S. Esposito, V. Maione, L. Russo, I. Baglivo, I. de Paola, D. Milardi, D. Diana, L. Zaccaro, P. V. Pedone, R. Fattorusso and C. Isernia, *Metallomics*, 2014, **6**, 96-104.

32. M. Palmieri, L. Russo, G. Malgieri, S. Esposito, I. Baglivo, A. Rivellino, B. Farina, I. de Paola, L. Zaccaro, D. Milardi, C. Isernia, P. V. Pedone and R. Fattorusso, *J Inorg Biochem*, 2014, **131**, 30-36.

Supplementary Informations

Table S1. pHis2 proton chemical shifts (ppm) in H_2O at 298 K.

	NH	αCH	βCH	Others
His1	-	4.07	3.22	C2 8.51; C4 7.28
Lys2	-	3.81	1.72	NHsc 8.14 ε 3.10 γ δ 1.35 1.20
β-Ala3	8.22	2.46	3.40	
Lys4	8.08	4.08	1.61	NHsc 8.14 NH2t 7.52, 7.00 ε 3.10 γ δ 1.35 1.20
His5	-	4.07	3.22	C2 8.51; C4 7.28

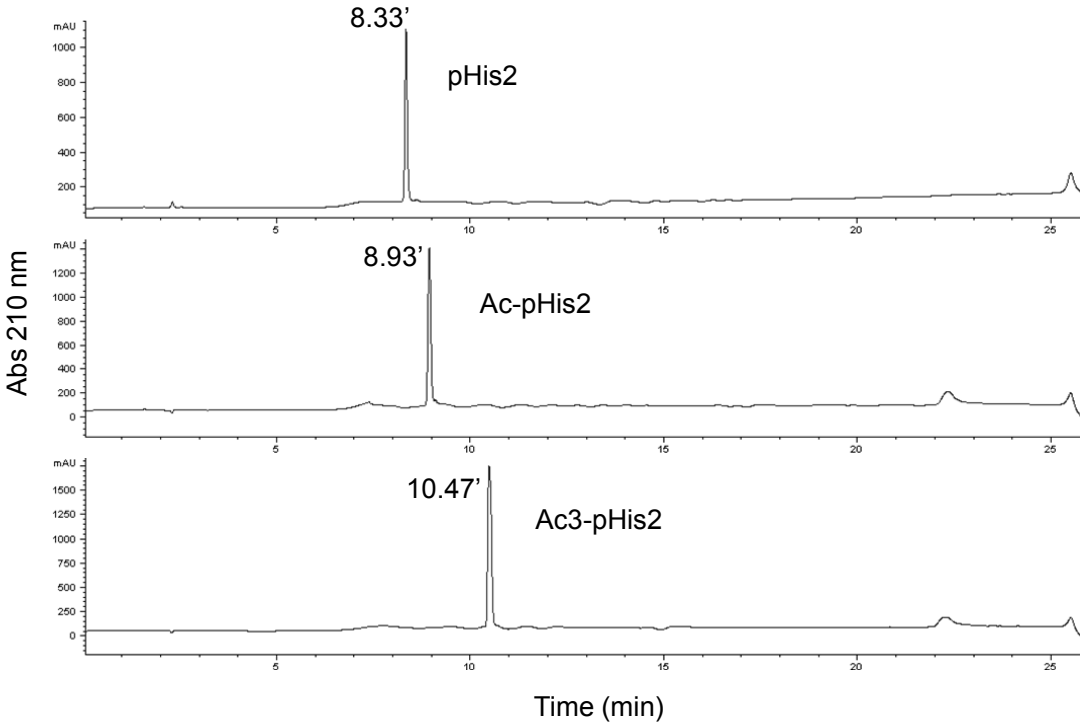

Figure S1: Analytical characterization by RP-HPLC of pHis2, Ac-pHis2 and Ac3-pHis2 peptides. Chromatograms were revealed reading the absorbance at 210 nm.

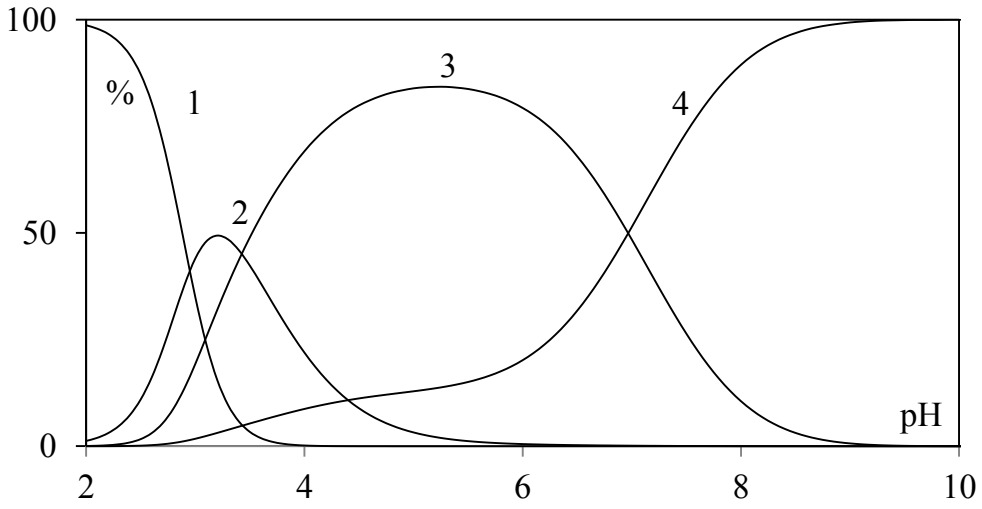

Fig.S2. Distribution diagram of Ga(III)–His system in 0.1 M $NaClO_4$ with $C_{Me} = 2.0 \cdot 10^{-3}$ M and $C_L = 4.0 \cdot 10^{-3}$ M (1: Ga^{3+}; 2: $Ga(OH)_2^+$, 3: $Ga(OH)_2His^+$; 4: $Ga(OH)_3$).

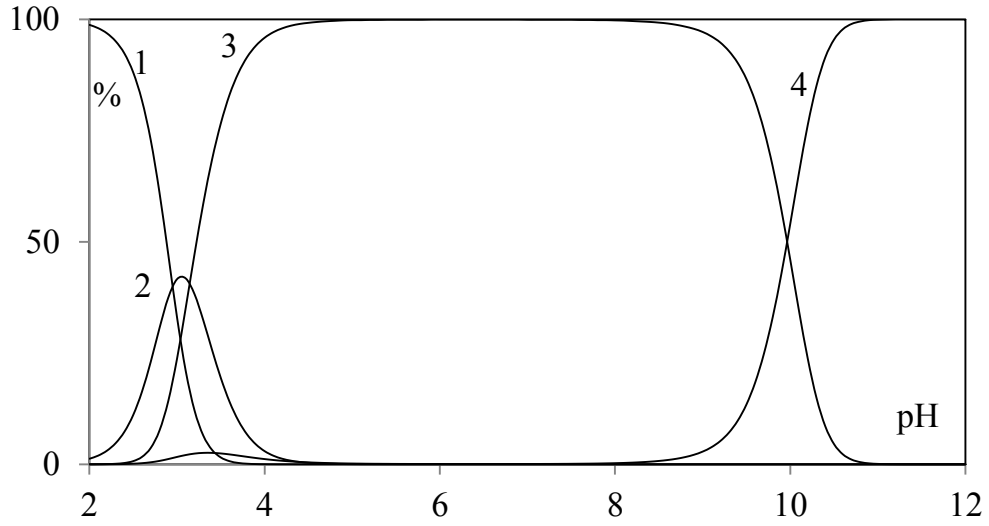

Fig.S3. Distribution diagram of Ga(III)–pHis2 system in 0.1 M $NaClO_4$ with $C_{Me} = 2.0 \cdot 10^{-3}$ M and $C_L = 4.0 \cdot 10^{-3}$ M (1: Ga^{3+}; 2: $Ga(OH)_2^+$, 3: $Ga(OH)_2H_3L^+$; 4: $Ga(OH)_3$).

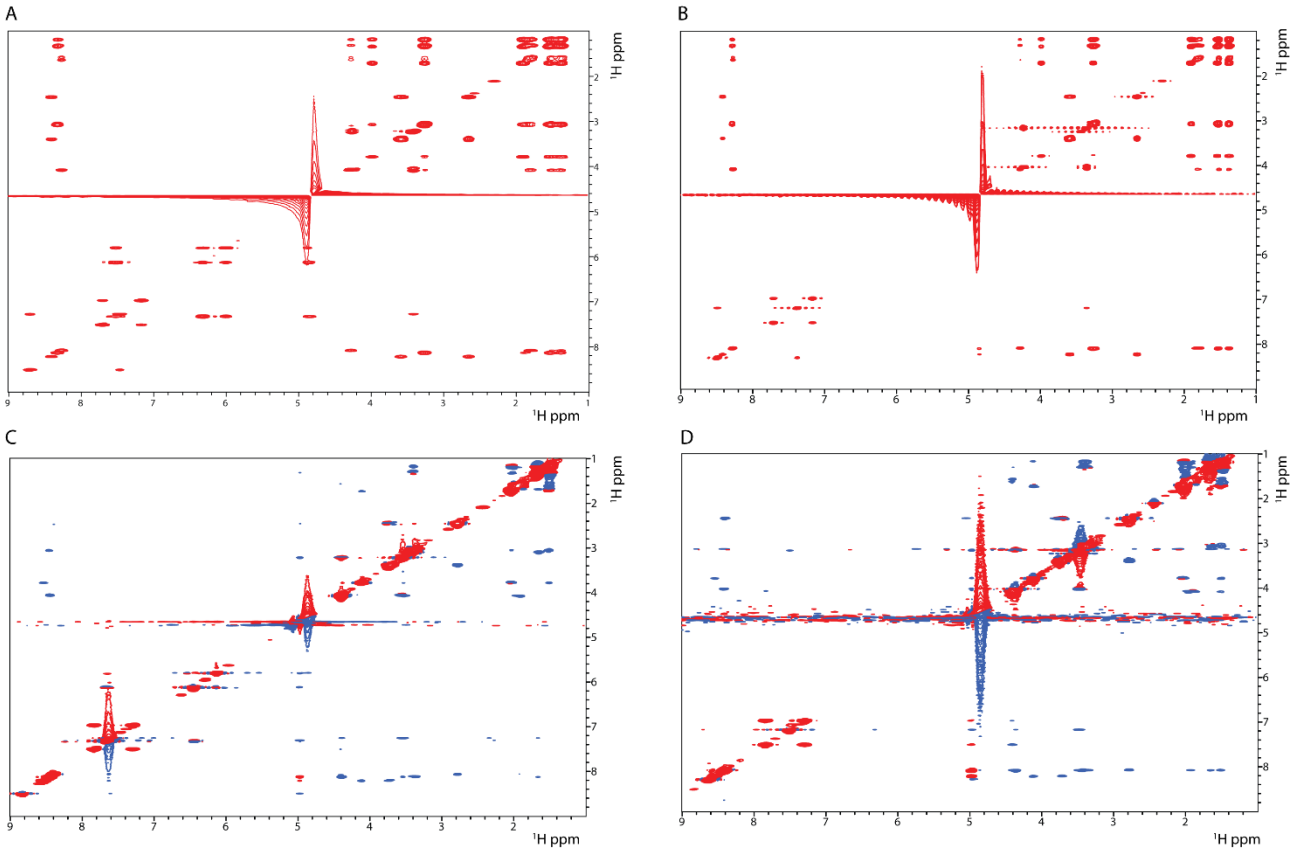

Fig.S4. ^{1}H-^{1}H TOCSY and NOESY spectra of the *fac*–$[Re(H_2O)_3(CO)_3]^+$–pHis2 (A and C, respectively) and of the Ga(III)–pHis2 complexes (B and D).

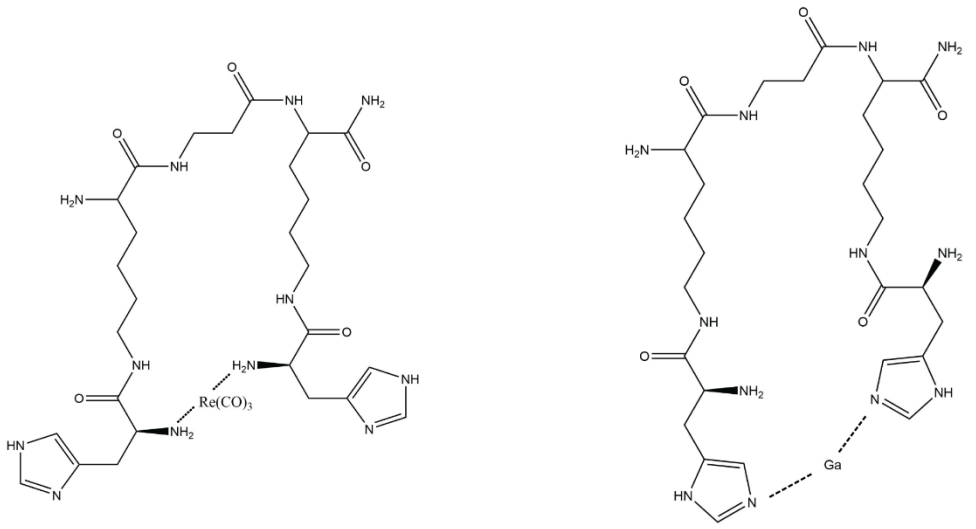

Fig.S5. Schematic representation of complex formed by pHis2 upon binding with *fac*–$[Re(H_2O)_3(CO)_3]^+$ (left) and with Ga(III) (right).